Reactivity of *trans*- and *cis*-Phenyldiazene Induced by the Internal Rotation of the Phenyl Group

Jenny Zevallos,[†] Jorge R. Letelier,[‡] and Alejandro Toro-Labbé*,[†]

Laboratorio de Química Teórica Computacional (QTC), Facultad de Química, Pontificia Universidad Católica de Chile, Casilla 306, Correo 22, Santiago, Chile, Departamento de Química, FCFM, Universidad de Chile, Casilla 2777, Santiago, Chile

Received: April 29, 2004; In Final Form: July 30, 2004

The reactivity of *trans*- and *cis*-phenyldiazene (H−N═N−C_6H_5) induced by the internal rotation of the phenyl group is studied through the characterization of the profiles of the energy, the chemical potential, the hardness, and the local electronic properties. Phenyldiazene presents two stable isomers when the phenyl group is trans or cis with respect to the hydrogen atom bonded to the second nitrogen. The trans isomer is planar, whereas in the cis isomer, the phenyl group is tilted by about 40° with respect to the molecular plane. The change of local reactivity indexes induced by the low-energy internal rotation motion explains the selectivity trend observed when *cis*-phenyldiazene is coordinated by a metallic complex.

1. Introduction

Monosubstituted diazenes (HNNR) are invoked as reactive intermediates in numerous important organic reactions including oxidations of arylhydrazines,[1] Wolff−Kishner reductions,[2] the McFadyen−Stevens conversion of carboxylic acids to aldehydes,[3] and reductive deaminations.[4] However, this elusive molecular class was not detected until 1965 when Kosower and Huang observed *trans*-phenyldiazene as the product of the decarboxylation of phenyldiazenecarboxylic acid.[5]

Phenyldiazene (HNNPh) is a reactive and thermally unstable species that usually decomposes at low temperatures with the loss of N_2[6] in contrast to the relatively inert disubstituted compound (like azobenzene); however, the coordination chemistry of this molecule is extensive, and thermally stable complexes of various metals including Pt, Ru, Os, Rh, Ir, Mn, Fe, and W are known.[7]

HNNPh presents two stable isomeric forms, the trans and cis conformations of the phenyl group with respect to the hydrogen bonded to the vicinal nitrogen (Figure 1). In the present work, the internal rotation of the phenyl (Ph) group around the N−C bond of both rotational isomers is studied with the aim of determining the change in the reactivity patterns induced by the internal rotation through the characterization of the profiles of the global and local reactivity descriptors. Global electronic properties such as electronegativity[8] (χ), molecular hardness[9] (η), and polarizability[10] (α) as well as the local Fukui index, which is used to characterize selectivity, are among the reactivity properties that will be discussed in this work.

For the sake of completeness, we briefly state the basic guidelines of reactivity principles that define the framework where these properties are analyzed. The principle of maximum hardness[11−13] (PMH) that establishes that "molecules reorder themselves in such a way that they are as hard as possible" and the minimum polarizability principle[14−17] (MPP) stating that "the natural direction of evolution of any system is toward a state of minimum polarizability" are two principles of chemical reactivity that will be useful in rationalizing the results.[17,18]

2. Theoretical Background

2.1. Global Reactivity Descriptors. In density functional theory (DFT), the chemical potential μ arises as the Lagrange multiplier associated with the condition that the electronic density integrates to N, the total number of electrons of the system;[19] it is defined as

$$\mu = \left(\frac{\partial E}{\partial N}\right)_{v(r)} \tag{1}$$

where $v(r)$ is the external potential due to the nuclei of an N-electron system with total energy E. The link between DFT and classical chemistry is achieved by making $\mu = -\chi$, where χ is the electronegativity.[8] Physically, μ characterizes the escaping tendency of electrons from an equilibrium system.

However, hardness is defined as[20,21]

$$\eta = \frac{1}{2}\left(\frac{\partial^2 E}{\partial N^2}\right)_{v(r)} \tag{2}$$

Hardness is the resistance of the system toward a reordering of the electron density.[11,19−22] Note that μ and η are the responses of the system when N is varied for a fixed $v(r)$.

Owing to the discontinuity of the derivatives of eqs 1 and 2, a three-point finite difference interpolation of the energy for the N, $N + 1$, and $N - 1$ electron systems[21,23] is used; this leads to the following working expressions for μ and η

$$\mu \approx -\left(\frac{I + A}{2}\right) \approx \frac{\epsilon_l + \epsilon_h}{2} \tag{3}$$

$$\eta \approx \left(\frac{I - A}{2}\right) \approx \frac{\epsilon_l - \epsilon_h}{2} \tag{4}$$

where I is the first ionization potential and A is the electron affinity. Subsequent use of Koopman's theorem[24] ($I \approx -\epsilon_h$ and

* Corresponding author. E-mail: atola@puc.cl.
† Pontificia Universidad Católica de Chile.
‡ Universidad de Chile.

10.1021/jp040321n CCC: $27.50
Published on Web 10/26/2004

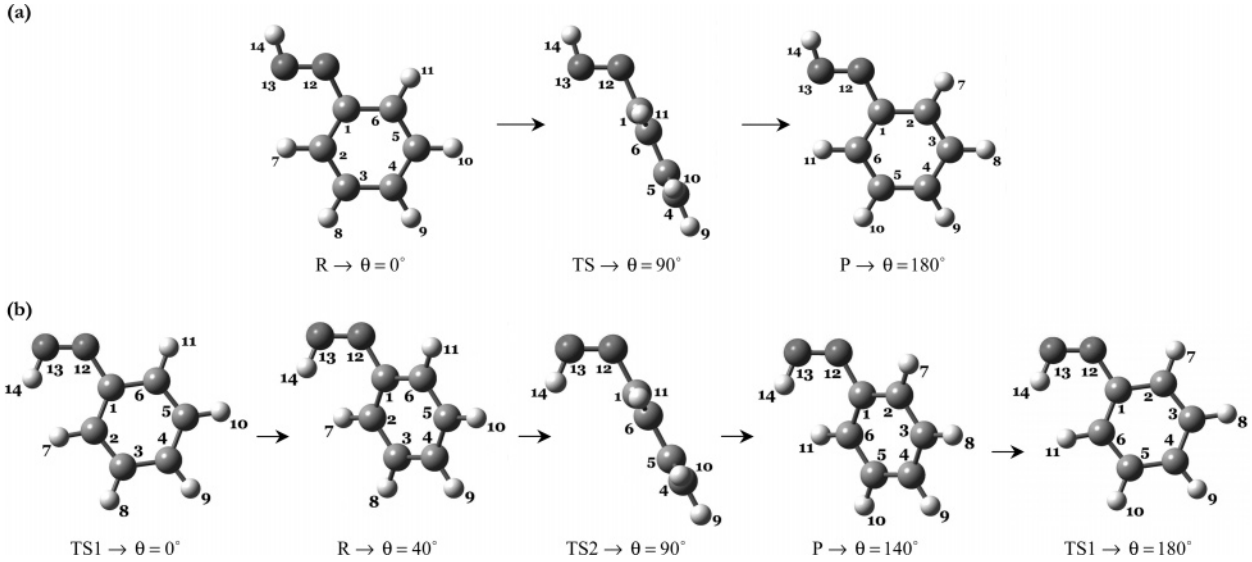

Figure 1. Schematic picture of the internal rotation of the Ph group in (a) *trans*-phenyldiazene and (b) *cis*-phenyldiazene.

$A \approx -\epsilon_l$) allows us to express μ and η in terms of the energies of frontier molecular orbitals HOMO (ϵ_h) and LUMO (ϵ_l).

The electrophilicity index[25] (ω) is a measure of the energy stabilization of a system when it is saturated by the electronic charge coming from the surroundings; it is defined as

$$\omega = \frac{\mu^2}{2\eta} \tag{5}$$

To complete the picture of the response of the system when changing the basic variables N and $\nu(r)$, we analyzed the polarizability (α), which is used to understand the behavior of the system when changing $\nu(r)$ at constant N. In this context, we analyzed the arithmetic average of the diagonal components of the tensor[10,17,26]

$$\alpha \equiv \langle \alpha \rangle = \frac{1}{3}(\alpha_{xx} + \alpha_{yy} + \alpha_{zz}) \tag{6}$$

Because the polarizability is expected to be inversely proportional to the hardness,[11,27] a highly polarized system is expected to be more reactive as stated by the MPP.[13,14,16−18]

2.2. Local Reactivity Descriptors. The most important local descriptor of site selectivity is the Fukui function[28] (FF), which is defined as follows:

$$f(r) = \left(\frac{\delta\mu}{\delta\nu(r)}\right)_N = \left(\frac{\partial\rho(r)}{\partial N}\right)_{\nu(r)} \tag{7}$$

Three types on FFs can be defined[28] on the basis of the discontinuity of the $\rho(r)$ versus N curve:[29]

$$f^+(r) \cong \left(\frac{\partial\rho(r)}{\partial N}\right)^+_{\nu(r)} = [\rho_{N+1}(r) - \rho_N(r)] \approx \rho_l(r) \tag{8}$$

for nucleophilic attack,

$$f^-(r) \cong \left(\frac{\partial\rho(r)}{\partial N}\right)^-_{\nu(r)} = [\rho_N(r) - \rho_{N-1}(r)] \approx \rho_h(r) \tag{9}$$

for electrophilic attack, and

$$f^\circ(r) \cong \left(\frac{\partial\rho(r)}{\partial N}\right)^\circ_{\nu(r)} = \frac{1}{2}[f^+(r) + f^-(r)] = \frac{1}{2}[\rho_l(r) + \rho_h(r)] \tag{10}$$

for radical attack. In the above equations, the FFs are related to the frontier molecular orbitals LUMO and HOMO through their respective electronic densities $\rho_l(r)$ and $\rho_h(r)$.[30] These are expressed in terms of the atomic basis functions[31] $\{\chi_\mu\}$ and then condensed to atom k, thus giving

$$f_k^+ = \sum_{\mu\in k}[|c_{\mu l}|^2 + \sum_{\nu\neq\mu} c^*_{\mu l}\, c_{\nu l} S_{\mu\nu}] \tag{11}$$

for a nucleophilic attack and

$$f_k^- = \sum_{\mu\in k}[|c_{\mu h}|^2 + \sum_{\nu\neq\mu} c^*_{\mu h}\, c_{\nu h} S_{\mu\nu}] \tag{12}$$

for an electrophilic attack. The above equations satisfy their respective normalization conditions, namely,

$$\sum_k f_k^+ = 1 \text{ and } \sum_k f_k^- = 1 \tag{13}$$

3. Computational Details

Full geometry optimizations along the torsional reaction coordinate with the constraint that the aromatic ring remains planar were carried out at the HF/6-311G** level using the Gaussian98/03 package,[32] polarizability calculations along the reaction coordinate were performed using Pople and Sadlej's[33] basis sets, and vibrational frequency calculations were performed to check the nature of the critical points along the reaction coordinate. Chemical potential and hardness were calculated from the frontier orbitals energies using eqs 3 and 4, respectively; f_k^- was obtained by using eq 12. The profiles of the different properties were generated through calculations every 10° along the torsional angle θ. All quantities analyzed here are relative to the reactant value so that for a given property Q, $\Delta Q(\theta) = Q(\theta) - Q(\theta_R)$ where θ_R represents the position of the reactant stable isomer, which was found at $\theta_R = 0°$ for the trans isomer and at $\theta_R = 40°$ for the cis isomer.

4. Results and Discussion

Sketches of the conformational reactions that were studied in this paper are displayed in Figure 1. Although not shown here, we note that the geometrical parameters of *trans*- and *cis*-HNNPh isomers do not show noticeable changes along the

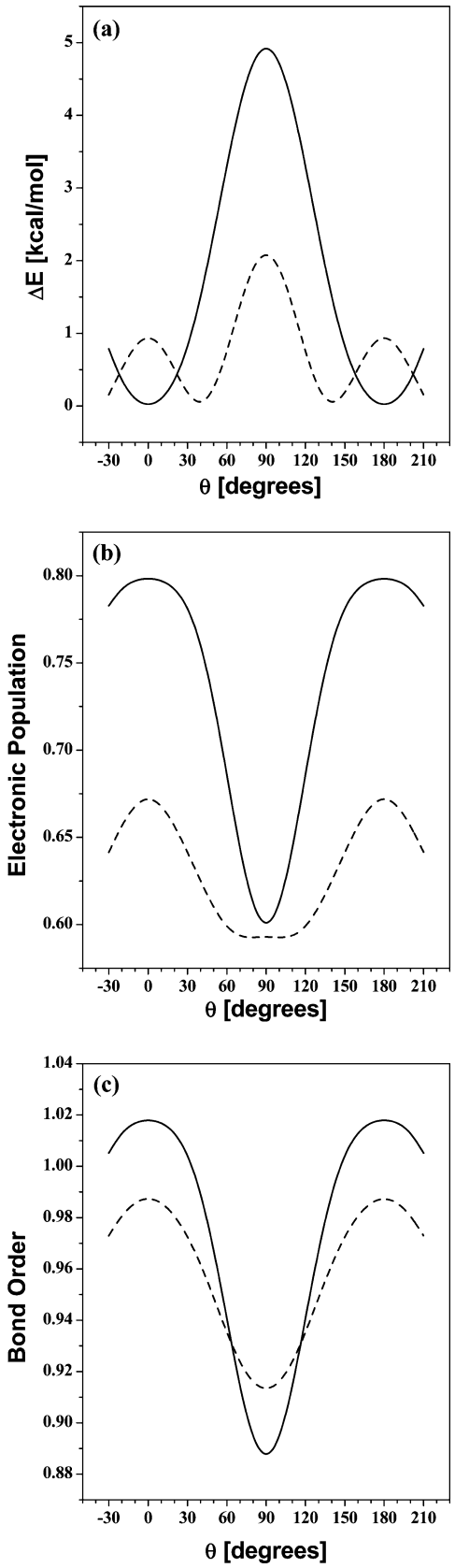

Figure 2. (a) ΔE, (b) electronic population of the N−C bond, and (c) N−C bond order profiles for the internal rotation of the Ph group in *trans*-phenyldiazene (—) and *cis*-phenyldiazene (- - -).

torsional motion, although the bond angles may change by a few degrees.

4.1. Energy Profile and Rotational Barriers. The energy profiles ($\Delta E(\theta)$) for the rotation of the phenyl group in both isomers that were calculated at the HF/6-311G** level are shown in Figure 2a. The expected symmetry with respect to $\theta = 90°$ is reached in both cases, although the trans and cis profiles are qualitatively and quantitatively different. The energy profile of *trans*-HNNPh presents a single energy barrier of about 5 kcal/mol at $\theta = 90°$; we note that the internal rotation of the phenyl group does not produce a new stable conformation besides the one found at $\theta = 0°$, and the energy barrier at $\theta = 90°$ separates the two symmetric conformations. In *cis*-HNNPh, the energy profile is characterized by two barriers, one of about 1 kcal/mol at $\theta = 0°$ (TS1) and another of 2 kcal/mol at $\theta = 90°$ (TS2).

TABLE 1: Energy Barriers for the Internal Rotation of the Ph Group in *trans*- and *cis*-Phenyldiazene[a,b]

method/6-311G**	*trans*-HNNPh $\Delta E^{\ddagger}$ ($\theta = 90°$)	*cis*-HNNPh $\Delta E^{\ddagger}$ ($\theta = 0°$)	*cis*-HNNPh $\Delta E^{\ddagger}$ ($\theta = 90°$)
HF	4.99	0.98	2.14
	4.58	0.79	1.82
Xα	6.94	0.29	3.95
	6.45	0.04	3.67
XαVWN	7.28	0.26	4.27
	6.80	0.00	3.99
PW91	6.32	0.17	3.44
	5.85	−0.05	3.18
B3LYP	5.96	0.33	3.03
	5.50	0.13	2.75
MP2	4.43	1.21	2.43
	4.09	0.86	2.01
QCISD	4.07	1.06	2.07

[a] Energies are in kcal/mol. [b] Second entry includes ZPE when available.

With the aim of assessing these results, we have performed extra calculations using different DFT approximations:[34] the Xα functional for exchange, Xα with the Vosko−Wilk−Nusair functional for correlation (XαVWN), the Perdew−Wang 91 functional for exchange with the Perdew−Wang 91 functional for correlation (PW91), and Becke's three-parameter hybrid functional for exchange with the Lee−Yang−Parr functional for correlation (B3LYP). Post-HF calculations have also been performed: the Møller−Plesset perturbation theory[35] up to second order (MP2) and the quadratic configuration interaction including singles and doubles[36] (QCISD). In all cases, the molecular structures were fully optimized. The results of these calculations are shown in Table 1. It is interesting that at the DFT level (all functionals) only the barriers at $\theta = 90°$ are energetically signficant at room temperature; however, the inclusion of the correlation energy through MP and QCI calculations confirms the existence of the potential barrier at $\theta = 0°$ in *cis*-HNNPh that was detected by the Hartree−Fock calculations. Furthermore, the addition of the zero-point energy (ZPE) correction confirms the above observation.

Surprisingly, the DFT calculations overestimate the barrier height with respect to HF, QCISD, and the reference MP2 results that have long been recognized for giving good estimates for energy barriers.[37] This is probably due to the self-interaction error that is contained in the classical Coulomb energy of the Kohn−Sham Hamiltonian, which is only partially canceled by the exchange-correlation term.[21,38] Moreover, the decomposition of the self-interaction energy into correlation and exchange parts in general shows that the exchange self-interaction error is the main component of the energy-barrier error.

Energy Barriers and Bond Population Analysis. All calculations show that the energy barrier at $\theta = 90°$ in *trans*-HNNPh is about twice the corresponding barrier in *cis*-HNNPh. This result can be explained by analyzing the electronic population

TABLE 2: Reference Values for Global Properties of Stationary Points in the Internal Rotation of the Ph Group in *trans*- and *cis*-Phenyldiazene[a]

	0°	40°	90°	140°	180°
E (au)	−339.624521		−339.616573		−339.624521
	−339.611153	−339.612712	−339.609295	−339.612712	−339.611153
μ (kcal/mol)	−79.67		−66.56		−79.67
	−85.18	−80.39	−72.63	−80.39	−85.18
η (kcal/mol)	131.74		141.99		131.74
	132.83	136.16	142.85	136.16	132.83
α (au)	217.8880		210.4440		217.8880
	215.9650	212.8290	209.2480	212.8290	215.9650
DM (Debye)	0.64		0.18		0.64
	3.69	3.52	3.33	3.52	3.69

[a] First entry corresponds to *trans*-HNNPh, and second entry, to *cis*-HNNPh.

and bond order of the N−C bond around which the rotation is performed. The computational definition for the bond order between two atoms has been proposed by Mayer[39] as an extension of Mulliken population analysis. In Figure 2b and c, the profiles of these properties are shown where it is apparent that the N−C bond in *trans*-HNNPh is stronger than that in *cis*-HNNPh; therefore, the rotation in *trans*-HNNPh is more hindered than it is in *cis*-HNNPh. In *trans*-HNNPh, the N−C bond population changes drastically from a broad maximum to a sharp minimum, with an overall variation of about 0.20 electron; the bond order change is very similar to that of the population, and the overall variation is about 0.13 electron. In contrast to this, in *cis*-HNNPh, the bond electronic population changes in a more subtle way from a somewhat sharp maximum to a broad minimum at TS2. It is interesting that the bond population of *cis*-HNNPh cannot help to identify the TS2 conformation because in this region the bond population reaches a plateau because of the fact that the structures at the proximities of the TS are very similar.

4.2. Global Electronic Properties. Global properties for the stationary points of both isomers are listed in Table 2, and the profiles of various global properties are displayed in Figure 3.

Chemical Potential and Molecular Hardness. It is readily seen in Figure 3 that the PMH does not hold in *trans*-HNNPh, whereas it is partially fulfilled in the TS1 region of *cis*-HNNPh. The $\Delta\mu$ and $\Delta\eta$ profiles of the *trans*-HNNPh and *cis*-HNNPh isomers are very similar and show a considerable variation along θ. In *trans*-HNNPh, $\Delta\eta(\theta)$ presents a minimum at the stable conformation ($\theta = 0°$) and a maximum at the TS ($\theta = 90°$) in contrast with what is expected from the PMH. In *cis*-HNNPh, a minimum of $\Delta\eta(\theta)$ at TS1 and a maximum at TS2 indicate a partial fulfillment of the PMH, only at the TS1 region; the strong variations observed in the chemical potential (Figure 3a) may explain the failure of the PMH, although it has been shown that the PMH may fail even though the chemical potential remains constant along the reaction coordinate.[40]

The strong variation in the chemical potential along θ indicates that an important rearrangement of the electronic density occurs during the internal rotation. In both isomers, $\Delta\mu$ presents a maximum at $\theta = 90°$ that is probably due to an extra electronic delocalization produced by the overlap between the π electronic cloud of the ring and the lone pair of the nitrogen.

A simple model to rationalize the charge flow along a reaction coordinate consists of assuming that an ensemble of molecules are distributed along the reaction coordinate and have their own $E(\theta)$, $\mu(\theta)$, and $\eta(\theta)$ values. Then the amount of charge flow is proportional to the difference in the chemical potential of the molecules at different conformations,[41] and an estimate of the intramolecular charge transfer (ΔN) when going from θ_1, a reference conformation, to θ can be obtained through the following expression that was borrowed from the intermolecular charge-transfer model proposed elsewhere[19,21,41]

$$\Delta N(\theta) = \frac{1}{2}\left[\frac{\mu(\theta) - \mu(\theta_1)}{\eta(\theta) + \eta(\theta_1)}\right] \tag{14}$$

When calculating ΔN with this expression and taking the stable conformation to be the reference (θ_1), we observe that in both isomers the TS ($\theta = 90°$) presents a maximum charge transfer that is an indicative of the charge delocalization discussed earlier (Figure 3c).

Electrophilicity Index, Electrostatic Potential, and Dipole Moment. In Figure 3d and e, the electrophilicity index ($\Delta\omega$) and the dipole moment (ΔDM) profiles are displayed. In both isomers, the profiles show a maximum when the molecules are planar ($\theta = 0°$) and a minimum at the TS when $\theta = 90°$. The minimum in ω confirms the above-mentioned extra electronic delocalization. However, although the change in DM is very small, it does allow us to confirm the rearrangement of the charge distribution at the TS in the sense mentioned previously.

In Figure 4a and b, the HF/6-311G** electrostatic-potential surfaces of the stationary points of *trans*-HNNPh and *cis*-HNNPh are displayed. We observe that at $\theta = 90°$ there is a maximum overlap between the π electronic cloud of the ring and the lone pair electrons of the nitrogen. This result is consistent with the already-discussed $\Delta\mu$ and ΔN profiles (Figure 3).

Polarizability. The polarizability is a measure of the change that takes place in the electronic density due to the presence of an external electric field. In Figure 3f, the polarizability profiles ($\Delta\alpha$) of both isomers are presented, and $\Delta\alpha$ shows a maximum at $\theta = 0°$ and a minimum at $\theta = 90°$ in contrast with what is expected from the MPP. In *cis*-HNNPh, this result indicates only a partial fulfillment with the MPP in the case of TS1.

Although we do not explicitly show the results here, the polarizability was also calculating using Sadlej's[33] basis set, which has been recognized as appropriate to reproduce electric properties. The results show the same trends observed in Figure 3f when using Pople's basis set.

4.3. Local Properties. Because phenyldiazene is a nucleophile, the analysis of the Fukui function for an electrophilic attack provides information about the local reactivity. We

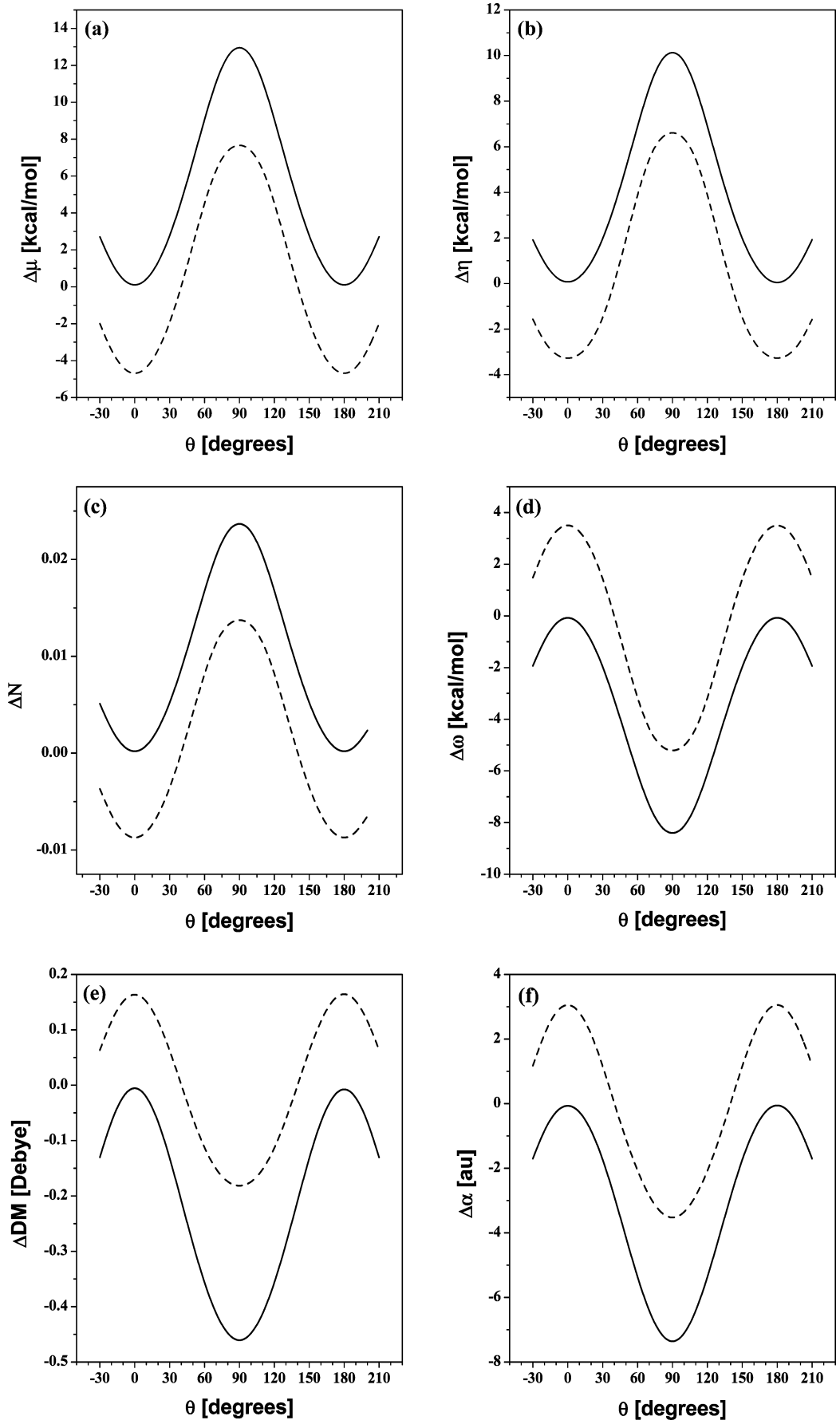

Figure 3. (a) $\Delta\mu$, (b) $\Delta\eta$, (c) ΔN, (d) $\Delta\omega$, (e) ΔDM, and (f) $\Delta\alpha$ profiles for the internal rotation of the Ph group in *trans*-phenyldiazene (—) and *cis*-phenyldiazene (- - -).

observe in Figure 5 that for both isomers the most reactive site for an electrophilic attack is C_4 (the atom located at the para

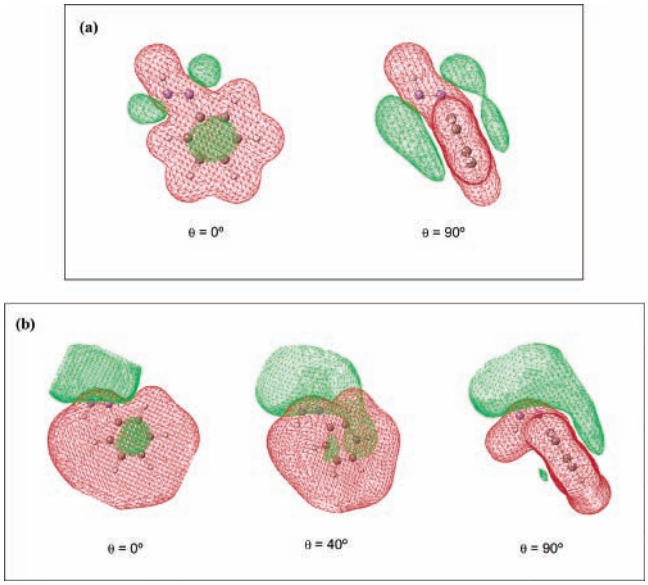

Figure 4. Electrostatic potential surfaces for stationary points at the HF/6-311G** level in (a) *trans*-phenyldiazene and (b) *cis*-phenyldiazene, with SCF total densities of 0.02 and 0.0125, respectively.

position) when the Ph group is perpendicular to the molecular plane ($\theta = 90°$), but when this group is on the plane ($\theta = 0°$), the most reactive sites are now C_1 (the atom directly bonded to the N atom of the azo group) and C_4. Both atoms present similar values of f_k^-, although C_1 presents an f_k^- value that is slightly larger than that of C_4. In the case of nitrogen atoms, we observe that independent of the isomer when the molecule is planar N_{12} is less nucleophilic than N_{13} and when the Ph group is perpendicular to the molecular plane the situation is reversed.

An interesting feature of Figure 5 is that important changes in the local reactivity indexes are induced at quite a small energy cost. We observe in Figure 5b and d that the reactivity pattern presented by the nucleophilic Fukui function of the nitrogens can be inverted quite easily by the torsional motion, $f_{N_{12}(N_{13})}^-$ increases (decreases) up to 7 or 8 times the original value at $\theta = 0°$; this change is associated with an energetic cost of just few kilocalories per mole (Figure 2a).

4.4. *cis*-HNNPh as a Ligand in a Metallic Complex. To illustrate the use of local reactivity indexes, we consider the coordination of *cis*-HNNPh with an electrophile so that the nucleophilic Fukui function (f^-) of the atoms in the molecule may provide the information that is necessary to determine the

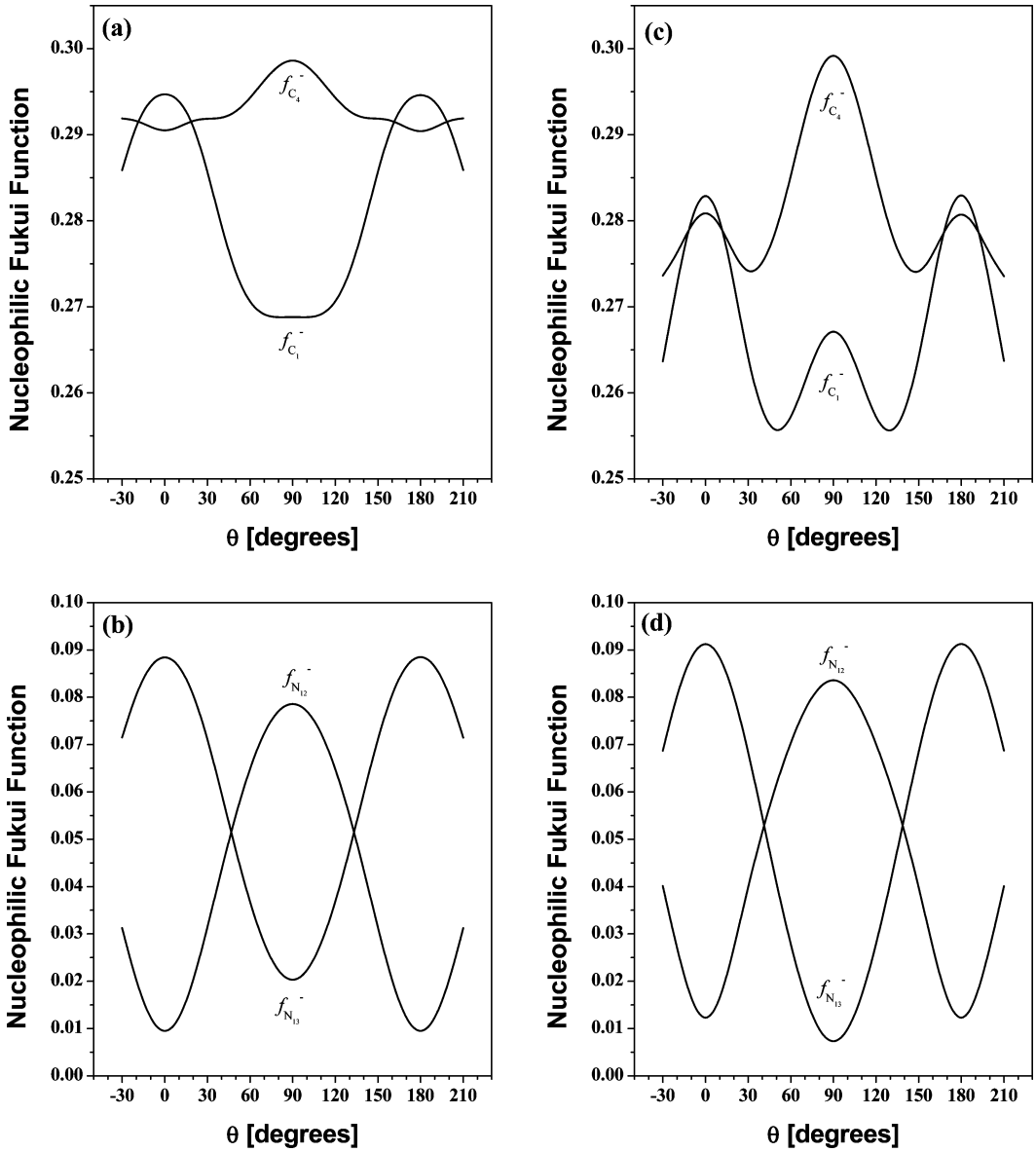

Figure 5. f_k^- profile for the internal rotation of the Ph group in (a) and (b) *trans*-phenyldiazene and (c) and (d) *cis*-phenyldiazene.

specific site of coordination. Figure 5d indicates that both nitrogen atoms present an equal amount of nucleophilic power at the stable conformation at $\theta = 40°$. However, it has been reported that N_{13} is the preferred site for coordination of a metallic complex where the phenyldiazene ligand adopts the cis conformation to accommodate the two bulky groups, a ruthenium (or platinum) metallic complex and the phenyl group, so that they arrange themselves to be trans to each other;[43] the metal is then coordinated to the phenyldiazene ligand through N_{13}.

Experimental evidence[43] indicates that optimum conjugation between the N═N unit and the phenyl group is needed to favor the entrance of the metallic complex; to fulfill this requirement, the $N_{12}C_1C_2$ angle must be equal to 120°, and the $N_{13}N_{12}C_1C_2$ dihedral angle should be zero. However, the very short $H_{14}\cdots H_7$ distance of 1.75 Å (the experimental average distance found in several complexes) would become even shorter (about 1.46 Å) under these idealized conditions, thus maximizing the electrostatic repulsion. It has been observed[43] that the $N_{13}N_{12}C_1C_2$ dihedral angle increases to about 20° and the $N_{12}C_1C_2$ angle opens up to ~125°, thus significantly relieving the $H_{14}\cdots H_7$ repulsive interaction. Therefore, a compromise between the maximum conjugation together with an acceptable $H_{14}\cdots H_7$ repulsion is found when moving along θ from the stable conformation at $\theta = 40°$ toward the TS1, which requires quite a small amount of energy (Figure 2a). Note that at the low temperatures (0 °C) at which these compounds are prepared the TS1 barrier, although small, is still significant.

Figure 5d indicates that when going from $\theta = 40°$ to TS1 the torsional motion is accompanied by a splitting of the f^- associated with N_{12} and N_{13} so that the reactivity of the nitrogen atoms makes them distinguishable from each other. At $\theta = 20°$, N_{13} is a better nucleophile than N_{12} (Figure 5d), which indicates that the coordination of the metal with *cis*-HNNPh must occur through N_{13}, a result that is in agreement with the experimental evidence.[43]

5. Concluding Remarks

In this work, a theoretical study of the internal rotation of the phenyl group of trans and cis isomers of phenyldiazene has been presented. The process for *trans*-HNNPh exhibits a single barrier, whereas that for *cis*-HNNPh presents a double barrier. The energy barrier of *trans*-HNNPh is larger than that of *cis*-HNNPh because of a higher electronic population on the torsional bond.

The change of local reactivity indexes induced by the low-energy internal rotation motion explains the selectivity preference observed when *cis*-phenyldiazene is coordinated by a ruthenium (or platinum) metallic complex.

Acknowledgment. This work has been supported by FONDECYT through project nos. 1020534, 1040923, and 2010099 and by MECESUP through projects PUC-0004 and Red Química UCH-0116.

References and Notes

(1) Cram, D. J.; Bradshaw, J. D. *J. Am. Chem. Soc.* **1963**, *85*, 1108. Huyser, E. S.; Wang, R. H. S. *J. Org. Chem.* **1968**, *33*, 2901.

(2) Szmant, H. H.; Roman, M. M. *J. Am. Chem. Soc.* **1966**, *88*, 4034.

(3) McFadyen, J. S.; Stevens, T. S. *J. Chem. Soc.* **1936**, 584.

(4) Nickon, A.; Hill, A. S. *J. Am. Chem. Soc.* **1964**, *86*, 1152. Bumgardner, C. L.; Martin, K. H.; Freeman, J. P. *J. Am. Chem. Soc.* **1963**, *85*, 97. Doldouras, G. A.; Kollonitsch, J. *J. Am. Chem. Soc.* **1978**, *100*, 314.

(5) Kosower, E. M.; Huang, P. C. *J. Am. Chem. Soc.* **1965**, *87*, 4646. Kosower, E. M.; Huang, P. C. *J. Am. Chem. Soc.* **1968**, *90*, 2354. Kosower, E. M.; Huang, P. C. *J. Am. Chem. Soc.* **1968**, *90*, 2362. Kosower, E. M.; Huang, P. C. *J. Am. Chem. Soc.* **1968**, *90*, 2367.

(6) Kosower, E. M. *Acc. Chem. Res.* **1971**, *4*, 193. Kosower, E. M.; Tsuji, T. *J. Am. Chem. Soc.* **1971**, *93*, 1992.

(7) Parshall, G. W. *J. Am. Chem. Soc.* **1965**, *87*, 2133. Parshall, G. W. *J. Am. Chem. Soc.* **1967**, *89*, 1822. Albertin, G.; Antoniutti, S.; Lanfranchi, M.; Pelizzi, G.; Bordignon, E. *Inorg. Chem.* **1986**, *25*, 950. Diels, O.; Koll, W *Liebigs Ann. Chem.* **1925**, *443*, 262. Petredis, D.; Burke. A.; Balch. A. *J. Am. Chem. Soc.* **1970**, *92*, 428. Sellemann, D.; Böhle, E.; Waeber, M.; Huttner, G.; Zsolnai, L. *Angew. Chem., Int. Ed. Engl.* **1985**, *24*, 981. Sellemann, D.; Soglowek, W.; Knoch, F.; Moll, M. *Angew. Chem., Int. Ed. Engl.* **1989**, *28*, 1271. Ackermann, M. N.; Willett, R. M.; Barton, C. R.; Shewitz, D. B. *J. Organomet. Chem.* **1979**, *175*, 205. Ackermann, M. N.; Dobmeyer, D. J.; Hardy, L. C. *J. Organomet. Chem.* **1979**, *182*, 561. Sellemann, D.; Gerlach, R.; Jödden, K. *J. Organomet. Chem.* **1979**, *178*, 433. Sellemann, D.; Jödden, K. *Angew. Chem., Int. Ed. Engl.* **1977**, *16*, 464.

(8) Sen, K. D., Joegensen, C. K., Eds. *Electronegativity: Structure and Bonding*; Springer-Verlag: Berlin, 1987; Vol. 66. Pauling. L. *The Nature of Chemical Bond and the Structure of Molecules and Crystals; An Introduction to Modern Structural Chemistry*; Cornell University Press: Ithaca, NY, 1960.

(9) Pearson, R. G. *Hard and Soft Acids and Bases*; Dowden, Hutchinson and Ross: Stroudsberg, PA, 1973. Pearson, R. G. *Cord. Chem. Rev.* **1990**, *100*, 403. Sen, K. D., Mingon, D. M. P., Eds. *Chemical Hardness: Structure and Bonding*; Springer-Verlag: Berlin, 1993; Vol. 80. Pearson, R. G. *Chemical Hardness: Applications from Molecules to Solids*; Wiley-VCH Verlag GMBH: Weinheim, Germany, 1987. Pearson, R, G. *J. Am. Chem. Soc.* **1963**, *85*, 3533.

(10) McQuarrie, D. A.; Simon, J. D. *Physical Chemistry: A Molecular Approach*; University Science Books: Sausalito, CA, 1997. Maitlad, G. C.; Rigby, M.; Smith, E. B.; Waheham, W. A. *Intermolecular Forces: Their Origin and Determination*; Clarendon Press: Oxford, U.K., 1987.

(11) Pearson, R. G. *J. Chem. Educ.* **1987**, *64*, 561.

(12) Pearson, R. G. *Acc. Chem. Res.* **1993**, *26*, 250. Parr, R. G.; Chattaraj, P. K. *J. Am. Chem. Soc.* **1991**, *113*, 1854. Chattaraj, P. K.; Liu, G. H. *Chem. Phys. Lett.* **1995**, *273*, 171. Ayers, P. W.; Parr, R. G. *J. Am. Chem. Soc.* **2000**, *122*, 2010.

(13) Chattaraj, P. K. *Proc. India Natl. Sci. Acad., Part A* **1996**, *62*, 513.

(14) Chattaraj, P. K.; Sengupta, S. *J. Phys. Chem.* **1996**, *100*, 16126.

(15) Ghanty, T. K.; Ghosh, S. K. *J. Phys. Chem.* **1996**, *100*, 12295. Chattaraj, P. K.; Fuentealba, P.; Gómez, B.; Contreras, R. *J. Am. Chem. Soc.* **2000**, *122*, 348.

(16) Chattaraj, P. K.; Poddar, A. *J. Phys. Chem. A* **1998**, *102*, 9944. Chattaraj, P. K.; Poddar, A. *J. Phys. Chem. A* **1999**, *103*, 1274. Chattaraj, P. K.; Poddar, A. *J. Phys. Chem. A* **1999**, *103*, 8691.

(17) Chattaraj, P. K.; Fuentealba, P.; Jaque, P.; Toro-Labbé, A. *J. Phys. Chem. A* **1999**, *103*, 9307. Jaque, P.; Toro-Labbé, A. *J. Phys. Chem. A* **2000**, *104*, 995.

(18) Chattaraj, P. K.; Zevallos, J.; Peréz, P.; Toro-Labbé, A. *J. Phys. Chem. A* **2001**, *105*, 4272. Chattaraj, P. K.; Gurierrez-Oliva, S.; Jaque, P.; Toro-Labbé, A. *J. Phys. Chem. A* **2003**, *101*, 2841.

(19) Parr, R. G.; Donnelly, R. A.; Levy, M.; Palke, W. E. *J. Chem. Phys.* **1978**, *68*, 3801.

(20) Parr, R. G.; Pearson, R. G. *J. Am. Chem. Soc.* **1983**, *105*, 7512.

(21) Parr, R. G. *Density Functional Theory of Atoms and Molecules*; Oxford University Press: New York, 1989.

(22) Pearson, R. G. *J. Am. Chem. Soc.* **1985**, *107*, 6801. Parr, R. G.; Yang, W. *Annu. Rev. Phys. Chem.* **1995**, *46*, 701.

(23) Pearson, R. G. *Proc. Natl. Acad. Sci. U.S.A.* **1986**, *83*, 8440.

(24) Koopmans, T. A. *Physica* **1933**, *91*, 651.

(25) Parr, R. G.; von Szentpály, L.; Liu, S. *J. Am. Chem. Soc.* **1999**, *121*, 1922.

(26) Hohm, U. *J. Phys. Chem. A* **2000**, *104*, 8418. Gutiérrez-Oliva, S.; Jaque, P.; Toro-Labbé, A. *J. Phys. Chem. A* **2000**, *104*, 8955. Pérez, P.; Toro-Labbé, A. *J. Phys. Chem. A* **2000**, *104*, 1557. Pérez, P.; Toro-Labbé, A. *Theor. Chem. Acc.* **2001**, *105*, 422.

(27) Politzer, P. *J. Chem. Phys.* **1987**, *86*, 1072. Fuentealba, P.; Reyes, O. *J. Mol. Struct.: THEOCHEM* **1993**, *282*, 65. Ghanty, T. K.; Ghosh, S. K. *J. Phys. Chem.* **1993**, *97*, 4951.

(28) Parr, R. G.; Yang, W. *J. Am. Chem. Soc.* **1984**, *106*, 4049. Fukui, K. *Science* **1987**, *218*, 747.

(29) Perdew, J. P.; Parr, R. G.; Levy, M.; Balduz, J. L. *Phys. Rev. Lett.* **1982**, *49*, 1691.

(30) Senet, P. *J. Chem. Phys.* **1997**, *107*, 2516.

(31) Contreras, R.; Fuentealba, P.; Galván M.; Pérez, P. *Chem. Phys. Lett.* **1999**, *304*, 405.

(32) Frisch, M. J.; Trucks, G. W.; Schlegel, H. B.; Scuseria, G. E.; Robb, M. A.; Cheeseman, J. R.; Zakrzewski, V. G.; Montgomery, J. A., Jr.; Stratmann, R. E.; Burant, J. C.; Dapprich, S.; Millam, J. M.; Daniels, A. D.; Kudin, K. N.; Strain, M. C.; Farkas, O.; Tomasi, J.; Barone, V.; Cossi, M.; Cammi, R.; Mennucci, B.; Pomelli, C.; Adamo, C.; Clifford, S.; Ochterski, J.; Petersson, G. A.; Ayala, P. Y.; Cui, Q.; Morokuma, K.; Malick,

D. K.; Rabuck, A. D.; Raghavachari, K.; Foresman, J. B.; Cioslowski, J.; Ortiz, J. V.; Stefanov, B. B.; Liu, G.; Liashenko, A.; Piskorz, P.; Komaromi, I.; Gomperts, R.; Martin, R. L.; Fox, D. J.; Keith, T.; Al-Laham, M. A.; Peng, C. Y.; Nanayakkara, A.; Gonzalez, C.; Challacombe, M.; Gill, P. M. W.; Johnson, B. G.; Chen, W.; Wong, M. W.; Andres, J. L.; Head-Gordon, M.; Replogle, E. S.; Pople, J. A. *Gaussian 98*; Gaussian, Inc.: Pittsburgh, PA, 1998. Frisch, M. J.; Trucks, G. W.; Schlegel, H. B.; Scuseria, G. E.; Robb, M. A.; Cheeseman, J. R.; Montgomery, J. A., Jr.; Vreven, T.; Kudin, K. N.; Burant, J. C.; Millam, J. M.; Iyengar, S. S.; Tomasi, J.; Barone, V.; Mennucci, B.; Cossi, M.; Scalmani, G.; Rega, N.; Petersson, G. A.; Nakatsuji, H.; Hada, M.; Ehara, M.; Toyota, K.; Fukuda, R.; Hasegawa, J.; Ishida, M.; Nakajima, T.; Honda, Y.; Kitao, O.; Nakai, H.; Klene, M.; Li, X.; Knox, J. E.; Hratchian, H. P.; Cross, J. B.; Adamo, C.; Jaramillo, J.; Gomperts, R.; Stratmann, R. E.; Yazyev, O.; Austin, A. J.; Cammi, R.; Pomelli, C.; Ochterski, J. W.; Ayala, P. Y.; Morokuma, K.; Voth, G. A.; Salvador, P.; Dannenberg, J. J.; Zakrzewski, V. G.; Dapprich, S.; Daniels, A. D.; Strain, M. C.; Farkas, O.; Malick, D. K.; Rabuck, A. D.; Raghavachari, K.; Foresman, J. B.; Ortiz, J. V.; Cui, Q.; Baboul, A. G.; Clifford, S.; Cioslowski, J.; Stefanov, B. B.; Liu, G.; Liashenko, A.; Piskorz, P.; Komaromi, I.; Martin, R. L.; Fox, D. J.; Keith, T.; Al-Laham, M. A.; Peng, C. Y.; Nanayakkara, A.; Challacombe, M.; Gill, P. M. W.; Johnson, B.; Chen, W.; Wong, M. W.; Gonzalez, C.; Pople, J. A. *Gaussian 03*; Gaussian, Inc.: Pittsburgh, PA, 2003.

(33) Sadlej, A. J.; Urban, M. *J. Mol. Struct.: THEOCHEM* **1991**, *234*, 147.

(34) See for example: Levine, I. N. *Quantum Chemistry*; Prentice Hall: Upper Saddle River, NJ, 2000.

(35) Møller, C.; Plesset M. S. *Phys. Rev.* **1934**, *46*, 618. Szabo, A.; Ostlund, N. S. *Modern Quantum Chemistry*; McGraw-Hill: New York, 1989.

(36) Pople, J. A.; Head-Gordon, M.; Raghavachari K. *J. Chem. Phys.* **1987**, *87*, 5968.

(37) Hehre, W.; Radom, L.; Scheleyer, P.; Pople, J. *Ab Initio Molecular Orbital Theory*; John Wiley & Sons: New York, 1986. Gill, P. M. W. *Encyclopedia of Computational Chemistry*; John Wiley & Sons: New York, 1998.

(38) Baerends, E. J.; Gritsenko, O. V. *J. Phys. Chem. A* **1997**, *101*, 5383.

(39) Mayer, I. *Chem. Phys. Lett.* **1983**, *73*, 270.

(40) Torrent-Sucarrat, M.; Luis, J. M.; Duran, M.; Solà, M. *J. Am. Chem. Soc.* **2001**, *123*, 7951. Torrent-Sucarrat, M.; Luis, J. M.; Duran, M.; Solà, M. *J. Chem. Phys.* **2002**, *117*, 10561.

(41) Cadet, J.; Grand, A.; Moller, C.; Letelier, J. R.; Moncada, J. L. Toro-Labbé, A. *J. Phys. Chem. A* **2003**, *107*, 5343.

(42) Parr, R. G.; Bartolotti, L. J. *J. Am. Chem. Soc.* **1982**, *104*, 3801.

(43) Ittel, S. D.; Ibers, J. A. *J. Am. Chem. Soc.* **1974**, *96*, 4804. Haymore, B. L.; Ibers, J. A. *J. Am. Chem. Soc.* **1975**, *97*, 5369.